RED CELLS, IRON, AND ERYTHROPOIESIS

A mouse model of anemia of inflammation: complex pathogenesis with partial dependence on hepcidin

Airie Kim,[1,2] Eileen Fung,[1] Sona G. Parikh,[1] Erika V. Valore,[1] Victoria Gabayan,[1] Elizabeta Nemeth,[1] and Tomas Ganz[1,2]

[1]Department of Medicine, and [2]Department of Pathology, David Geffen School of Medicine at University of California, Los Angeles, Los Angeles, CA

Key Points

- An injection of heat-killed *Brucella abortus* in mice causes prolonged anemia with features similar to human anemia of inflammation.
- Ablation of hepcidin ameliorates anemia of inflammation in this model and allows faster recovery.

Anemia is a common complication of infections and inflammatory diseases, but the few mouse models of this condition are not well characterized. We analyzed in detail the pathogenesis of anemia induced by an injection of heat-killed *Brucella abortus* and examined the contribution of hepcidin by comparing wild-type (WT) to iron-depleted hepcidin-1 knockout (*Hamp*-KO) mice. *B abortus*–treated WT mice developed severe anemia with a hemoglobin nadir at 14 days and partial recovery by 28 days. After an early increase in inflammatory markers and hepcidin, WT mice manifested hypoferremia, despite iron accumulation in the liver. Erythropoiesis was suppressed between days 1 and 7, and erythrocyte destruction was increased as evidenced by schistocytes on blood smears and shortened red blood cell lifespan. Erythropoietic recovery began after 14 days but was iron restricted. In *B abortus*–treated *Hamp*-KO compared with WT mice, anemia was milder, not iron restricted, and had a faster recovery. Similarly to severe human anemia of inflammation, the *B abortus* model shows multifactorial pathogenesis of inflammatory anemia including iron restriction from increased hepcidin, transient suppression of erythropoiesis, and shortened erythrocyte lifespan. Ablation of hepcidin relieves iron restriction and improves the anemia. (*Blood*. 2014;123(8):1129-1136)

Introduction

Anemia of inflammation (AI) is a feature of a wide spectrum of inflammatory disorders, including connective tissue disease, infections, certain malignancies, and chronic kidney disease.[1] AI is typically a normocytic normochromic anemia with a shortened erythrocyte lifespan and suppressed erythropoiesis, despite adequate levels of circulating erythropoietin.[2] Perhaps the most consistent feature of AI is a derangement of systemic iron homeostasis characterized by hypoferremia with intact iron stores[1] and decreased availability of iron for erythrocyte production.

Hepcidin, a 25-amino acid peptide hormone produced primarily by hepatocytes,[3] is the principal regulator of iron homeostasis in health and during inflammation.[4] Excessive production of this hormone causes iron sequestration in macrophages and hypoferremia, as was shown in transgenic mice with hepcidin overexpression[5] and in the human genetic syndrome of hepcidin excess, iron-refractory iron-deficiency anemia due to mutations in matriptase-2/TMPRSS6.[6] Hepcidin acts by binding to ferroportin, the sole known cellular iron exporter, displayed on the surface of macrophages, hepatocytes, and the basolateral membranes of enterocytes. Hepcidin binding to ferroportin causes ferroportin endocytosis and degradation.[7] During inflammation or infection, hepcidin is strongly induced, largely by interleukin 6 (IL-6)[8] via the Janus kinase–signal transducer and activator of transcription pathway.[9-11] The extent to which increased production of hepcidin contributes to AI has not been directly tested by genetic ablation of hepcidin, in part because of the lack of robust mouse models of AI.

Multiple mouse models of inflammation have been developed to facilitate the testing of interventions in AI, but these models are limited by poor reproducibility and very mild anemia. Turpentine,[12,13] zymosan/lipopolysaccharide,[14] *Staphylococcus epidermidis*,[15] and complete Freund's adjuvant[15] treatments all cause AI in mice but with a mild anemia (hemoglobin [Hgb] $\geq$11 g/dL). Lipopolysaccharide injections alone have been shown to cause an acute inflammatory response with hepcidin elevation, but the hematologic effects have not been fully elucidated.[16] Cecal ligation and puncture is another potential method for studying AI, but its technical difficulty, variable outcomes, and associated morbidity make it cumbersome for routine use.

In response to the need for a robust mouse model of AI, we adapted and characterized a model of AI previously described by Sasu et al,[17] generated with a single intraperitoneal injection of heat-killed *Brucella abortus*. After a comprehensive examination of hematologic, iron, and inflammatory parameters of this model, we investigated the extent of hepcidin involvement in *B abortus*–induced AI by comparing wild-type (WT) C57BL/6 mice to hepcidin-1$^{-/-}$ mice on the same strain background.

Submitted August 18, 2013; accepted November 29, 2013. Prepublished online as *Blood* First Edition paper, December 19, 2013; DOI 10.1182/blood-2013-08-521419.

A.K. and E. F. contributed equally to this work.

The online version of this article contains a data supplement.

There is an Inside *Blood* commentary on this article in this issue.

The publication costs of this article were defrayed in part by page charge payment. Therefore, and solely to indicate this fact, this article is hereby marked "advertisement" in accordance with 18 USC section 1734.

Methods

Animal model of AI

All animal studies were approved by the Animal Research Committee at University of California, Los Angeles (UCLA). Only male mice were used in the study to avoid the effects of gender-related differences in iron parameters and hepcidin.[18] C57BL/6J mice were obtained from Charles River Laboratories (Wilmington, MA) or The Jackson Laboratories (Bar Harbor, ME). WT mice were maintained on a standard chow (~270 ppm iron; Harlan Teklad, Indianopolis, IN) until 6 weeks of age, and they were then switched to an adequate iron diet (50 ppm iron; Harlan Teklad) for 2 weeks before injection of *B abortus* or saline. The same iron-adequate diet was used through the remainder of the experiment. The dietary conditioning was applied because high iron content of standard chow maximally stimulates hepcidin expression and renders it unresponsive to inflammatory stimuli[8] and because dietary iron absorption in humans accounts for ~5% to 10% of the daily iron fluxes but as much as ~50% in mice fed standard chow.[19] High dietary iron absorption in mice may obscure the contribution of iron recycling by macrophages[20] and leads to progressive iron loading. Reducing the dietary iron content of mouse chow was designed to model iron fluxes of human homeostasis.

To induce AI, animals were injected intraperitoneally with 5×10^8 particles per mouse of heat-killed *B abortus* (strain 1119-3; US Department of Agriculture, Animal and Plant Health Inspection Service, National Veterinary Services Laboratories) as previously described.[17] Control mice were injected intreperitoneally with normal saline. Mice were euthanized over a time course (0-28 days), and blood, liver, spleen, pancreas, and kidney were collected at necropsy. For each time point, 8 saline and 8 *B abortus*–injected mice came from the same cohort and were processed simultaneously to minimize cohort-to-cohort variability, yielding 4 to 8 evaluable samples per group per time point.

For the study of the role of hepcidin in AI, we used male hepcidin-1 knockout mice (*Hamp1*$^{-/-}$ *or Hamp*-KO). *Hamp*-KO mice were originally provided to our laboratory by Dr Sophie Vaulont[21] and were backcrossed onto the C57BL/6 background as previously described[22] using marker-assisted accelerated backcrossing. For this study, *Hamp*-KO mice underwent dietary iron conditioning to prevent the development of iron overload and maintain iron levels comparable to those of WT mice. At weaning (3-4 weeks of age), *Hamp*-KO mice were placed on a low-iron diet (4 ppm) for 2 weeks followed by a 20 ppm iron diet for 2 weeks. This regimen allows for iron depletion without development of anemia. At 7 to 8 weeks of age, the mice were injected with *B abortus* or saline and switched to an adequate iron diet (50 ppm) to match the experimental conditions used for WT mice. *Hamp*-KO mice (3-8 evaluable per group and time point) were analyzed before and 7, 14, 21, and 28 days after *B abortus* or saline injection.

Measurement of iron parameters and erythropoietin

Serum iron and liver nonheme iron concentrations were determined by a colorimetric assay for iron quantification (Sekisui Diagnostics, Lexington, MA) as previously described.[19] Serum erythropoietin was measured by a solid-phase enzyme-linked immunosorbent assay according to the manufacturer's instructions (R&D, Minneapolis, MN).

Hematological studies

Complete blood counts were obtained with a HemaVet blood analyzer (Drew Scientific, Waterbury, CT). To assess iron-restricted erythropoiesis, zinc protoporphyrin (ZPP) was measured using a hematofluorometer (AVIV, Lakewood, NJ).

Reticulocytes were counted by flow cytometry. Blood (5 μL) was added to 1 mL of thiazole orange in phosphate-buffered saline with 0.1% sodium azide (PBS-azide; BD Bioscience; San Jose, CA) and incubated at room temperature for 1 to 3 hours. As an unstained control, blood was added to PBS-azide without thiazole orange. The percentage of red fluorescent reticulocytes (Retic %) was measured by flow cytometry at the UCLA Jonsson Comprehensive Cancer Center and Center for AIDS Research Flow Cytometry Core Facility that is supported by National Institutes of Health Awards CA-16042 and AI-28697, and by the Jonsson Comprehensive Cancer Center , the UCLA AIDS Institute, and the David Geffen School of Medicine at UCLA. Unstained controls were used to establish a gate to exclude background fluorescence. The results are expressed as the reticulocyte product index = Retic % × Hgb/14.46 g/dL, where 14.46 g/dL is a mean baseline Hgb level of healthy WT mice.

In vivo erythrocyte biotinylation

WT mice were injected intraperitoneally with saline or *B abortus*. On days 5 and 6, the mice were administered n-hydroxysuccinimide ester-(polyethylene glycol)4-biotin (NHS-PEG4-Biotin, 500 μg; Pierce, Rockford, IL) in PBS by retro-orbital injection. A total of 5 injections were given to maximize biotinylation efficiency. Over the subsequent 2 weeks, periodic retro-orbital bleeds (25-50 μL) were obtained to quantify the fraction of biotinylated erythrocytes (timeline indicated in supplemental Figure 1 on the *Blood* Web site). Each sample was divided into 2 aliquots: one to be labeled with anti–TER-119 (unstained) and the other with anti–TER-119 and streptavidin (stained). The labeling was performed as follows: 5 μL whole blood was diluted to 500 μL with Hank's balanced salt solution (Invitrogen, Carlsbad, CA) and 1% bovine serum albumin (Rockland, Gilbertsville, PA), and 2.5 μL rat anti-mouse TER-119-phycoerythrin added (BD Pharmingen, San Jose, CA). The stained group was also treated with 0.5 μL streptavidin-Alexa 488 (Molecular Probes, Eugene, OR). After incubation at room temperature for 1 hour, the samples were centrifuged and resuspended with Hank's balanced salt solution/bovine serum albumin. Flow cytometry was used to determine the percentage biotinylated erythrocytes (% stained – % unstained).

Serum hepcidin measurement

Mouse serum hepcidin-1 was measured by a sandwich enzyme-linked immunosorbent assay[23] (courtesy of B. Sasu and K. Cooke, Amgen, Thousand Oaks, CA). The assay was physiologically validated in our laboratory as described in the supplemental data.

RNA isolation and real-time quantitative polymerase chain reaction

Total RNA was isolated from liver and analyzed by real-time reverse transcriptase-polymerase chain reaction as described previously.[24] Primers are listed in supplemental Table 1.

Histocytopathology

Peripheral blood smears were performed using 10 μL whole blood at the time of necropsy, and prepared with Wright-Giemsa stain (Fisher, Hampton, NH). Formalin-fixed, paraffin-embedded liver and kidney tissues were stained with hematoxylin and eosin, periodic acid-Schiff, or Masson's trichrome stain at the UCLA Translational Pathology Core Laboratory. Immunoperoxidase staining with 1 μg/mL rat anti-mouse monoclonal antibody to the macrophage marker F4/80 (AbD Serotec, Kidlington, United Kingdom) was performed on deparaffinized sections after unmasking for 3 minutes with 20 μg/mL proteinase K. Sections were incubated overnight with the anti-F4/80 Mab solution, developed, and counterstained with hematoxylin, all using the Vectastain ABC kit (Vector Laboratories, Burlingame, CA).

Statistics

SigmaStat 11 was used for all statistical analyses (Systat Software, Point Richmond, CA). Normally distributed data were compared using the Student *t* test. Measurements that were not normally distributed were compared by the nonparametric Mann-Whitney *U* test. $P < .05$ was considered statistically significant, except for multiple comparisons where the Bonferroni correction was applied.

Results

B abortus–treated WT mice develop severe anemia with iron restriction

A single treatment with the inflammatory agent *B abortus* caused a dramatic hemoglobin decrease by 7 days with a nadir at 14 days

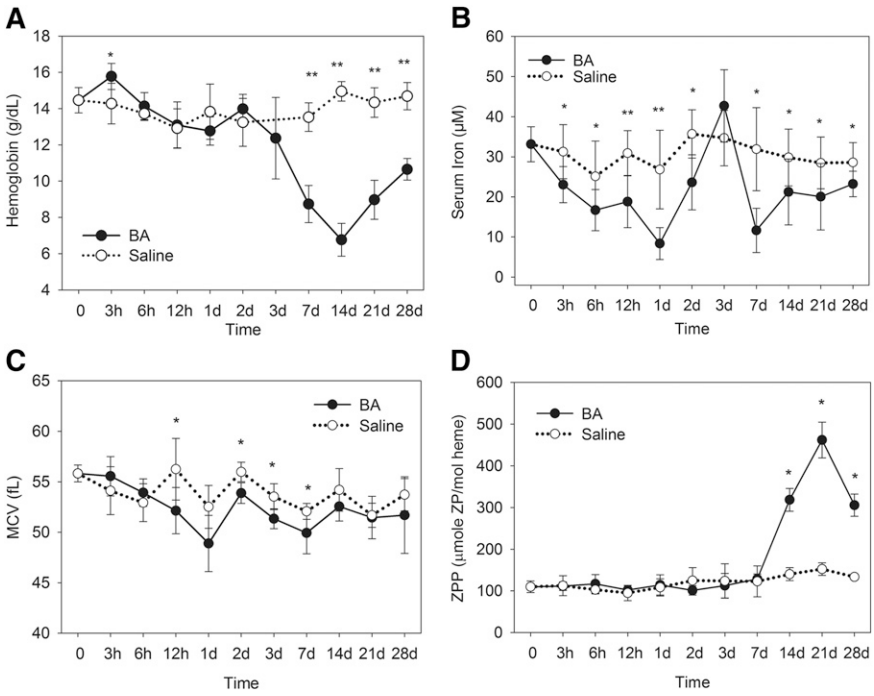

Figure 1. The *B abortus*–injected mice develop anemia and iron restriction. Compared with saline-injected mice, the *B abortus*–injected mice develop (A) a significantly lower hemoglobin by 7 days, with a nadir at 14 days and partial recovery by 28 days; (B) decreased serum iron concentrations through most time points, beginning at 3 hours, except for the transient underutilization of iron around day 3 during erythropoiesis suppression; (C) decreased MCVs within the first week; and (D) elevated ZPP levels between 14 and 28 days during the time of recovery from anemia. Saline and *B abortus* groups each included 4 to 8 evaluable male mice per time point. Means ± standard deviation (SD) are shown; $^*P < .05$ and $^{**}P < .001$ by Student *t* test or Mann-Whitney *U* test.

(Figure 1A; mean *B abortus* Hgb 6.8 g/dL vs saline Hgb 15.0 g/dL; $P < .001$ by Mann-Whitney *U* test). Afterward, there was a gradual but incomplete hemoglobin recovery by day 28 (*B abortus* Hgb 10.7 g/dL vs saline Hgb 14.7 g/dL; $P < .001$ by Student *t* test).

B abortus–injected mice rapidly developed a prolonged hypoferremia compared with saline-treated mice (Figure 1B). There was a transient increase in serum iron at 3 days, which was attributed to transient erythroid suppression and underutilization of circulating iron, as documented by subsequent data. However, all other time points showed a significant decrease in serum iron ($P < .05$ by Student *t* test). Additionally, within the first week, the mean corpuscular volume (MCV) was lower in the *B abortus*–treated mice, consistent with iron-restricted anemia[25] (Figure 1C). Later MCV measurements (14-28 days) in the *B abortus* group were not significantly different from the control group likely because of the increased number of larger stress reticulocytes in *B abortus* mice.

Erythrocyte ZPP levels were measured to further assess iron-restricted erythropoiesis (Figure 1D). When insufficient iron is available for erythropoiesis, increased amounts of zinc are incorporated into the protoporphyrin ring.[26] The *B abortus*–treated mice had comparable ZPP levels to untreated mice until a dramatic increase by 14 days (mean *B abortus* ZPP 319 μM/mole heme vs saline ZPP 140 μM/mole heme; $P < .001$ by Student *t* test), with an eventual peak at 21 days (*B abortus* ZPP 462 μM/mole heme vs saline ZPP 152 μM/mole heme; $P < .001$ by Mann-Whitney *U* test) and a partial recovery of *B abortus* ZPP by 28 days. As will be seen subsequently, the ZPP increase coincides with accelerated erythropoiesis during recovery from anemia.

B abortus–treated WT mice develop acute and chronic inflammation, with an early rise in hepcidin

We assessed the acute phase response to *B abortus* by measuring serum amyloid A1 (SAA1) messenger RNA (mRNA), which like hepcidin, is regulated by IL-6.[27] *B abortus*–treated mice developed an early-onset and persistent SAA1 mRNA elevation starting by 3 hours and lasting through 14 days (Figure 2A). In parallel with the increase in SAA1, hepcidin mRNA levels (Figure 2B) peaked at 6 hours with a greater than sixfold increase over their saline counterparts ($P < .05$ by Student *t* test), and serum hepcidin protein levels (Figure 2C; see the supplemental data for assay validation) were increased by greater than threefold at 6 hours ($P < .001$ by Student *t* test). Subsequently, hepcidin mRNA levels fell rapidly to levels similar to those of the saline-treated mice, perhaps responding to the developing hypoferremia (Figure 1B). However, normal hepcidin levels at 7 days are probably inappropriately high[28] considering the profound anemia and very high Epo production in *B abortus* mice (Figure 3) at that time point. By 14 days, *B abortus*–treated mice had significantly decreased hepcidin mRNA (<10% compared with saline controls; $P < .001$ by Student *t* test), presumably secondary to the known suppressive effect of increased erythropoiesis on hepcidin production.[28]

The *B abortus*–treated mice also developed chronic inflammation. By 7 days, the *B abortus*–treated mice developed a dramatic leukocytosis (*B abortus* white blood cell count [WBC] 29.6 thousand [K]/μL vs saline WBC 8.2 K/μL; $P < .001$ by Student *t* test), which incompletely resolved by day 28 (*B abortus* WBC 11.6 K/μL vs saline WBC 6.7 K/μL; $P < .05$ by Student *t* test; Figure 2D). Figure 2E demonstrates the hepatic perivascular infiltration of inflammatory cells in *B abortus*–treated mice at 7 days, which is contemporaneous with the increase in circulating white blood cells. By 14 days, hepatic granulomas were observed containing predominantly F4/80-positive macrophages (supplemental Figure 2A-B).

Suppression and recovery of erythropoietic response in *B abortus*–treated mice

By 7 days, serum erythropoietin levels were increased in *B abortus*–treated mice (Figure 3A; >12-fold increase over controls; $P < .001$ by Student *t* test), consistent with anemia (Figure 1A). By 21 days, as the anemia began to resolve, serum erythropoietin of the *B abortus*–treated mice started to fall (less than eightfold increase over controls; $P < .001$ by Mann-Whitney *U* test).

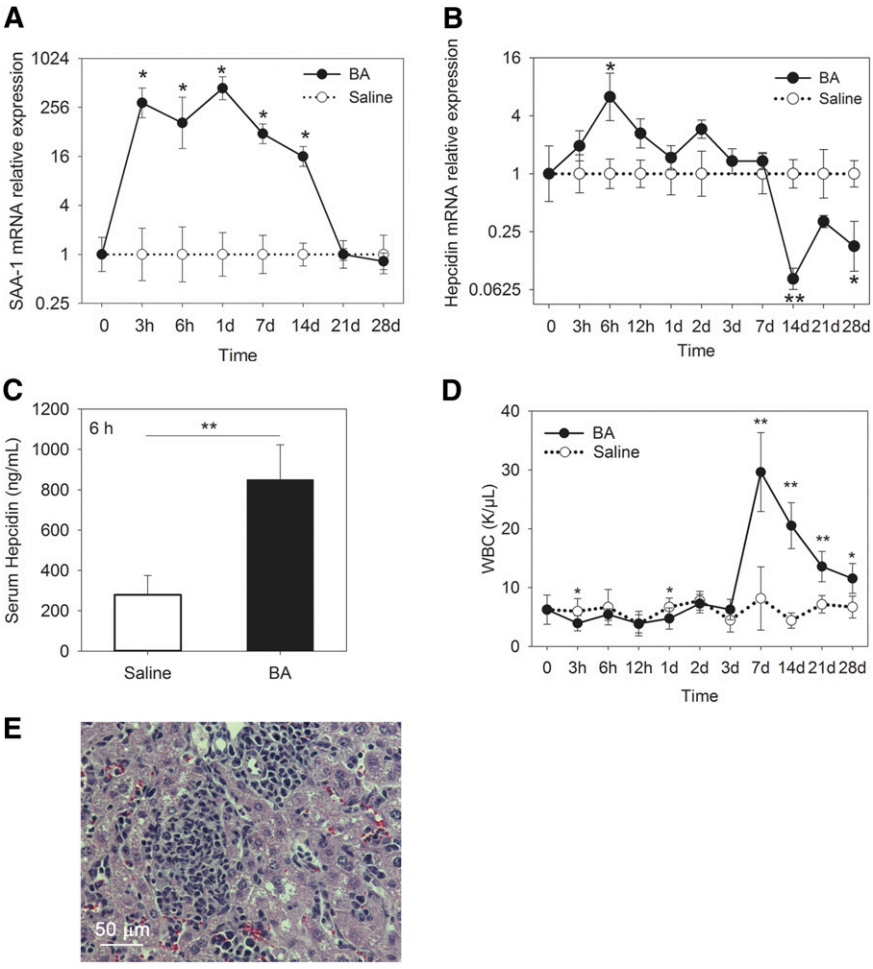

Figure 2. The *B abortus*–injected mice develop both acute and chronic inflammation, with an early rise in hepcidin mRNA. Compared with saline-injected mice, the *B abortus*–injected mice develop (A) increased SAA-1 mRNA by 3 hours, peaking at 1 day, and a gradual return to normal by 21 days; (B) increased hepcidin mRNA, with a peak at 6 hours, a slight but consistent increase through 7 days, followed by significant decrease at 14 and 28 days; (C) increased serum hepcidin protein at 6 hours; (D) increased WBCs by 7 days, with partial recovery by 28 days; and (E) hepatic perivascular infiltration of inflammatory cells by 7 days. (A-B) Means ± standard error, with each *B abortus*–treated group referenced to contemporaneous saline-treated group. (C-D) Means ± SD, $^*P < .05$ and $^{**}P < .001$ by Student *t* test or Mann-Whitney *U* test.

Reticulocyte measurements showed initial reticulocytosis at 3 hours after *B abortus* injection (Figure 3B), but this is likely due to massive release of stored near-mature reticulocytes rather than new production. During the first week, reticulocyte production decreased in *B abortus* mice (Figure 3B), indicating erythropoietic suppression. By 14 days, corresponding to the time of the highest erythropoietin levels and lowest hepcidin expression, reticulocytosis increased and peaked at 21 days (more than threefold increase over controls; $P < .001$ by Mann-Whitney *U* test). Because "stress" reticulocytes produced during stress erythropoiesis are significantly larger than mature erythrocytes, an increased percentage of reticulocytes effectively increased the red cell distribution width between days 14 and 28 (Figure 3C).

Shortened red blood cell lifespan and increased red blood cell hemolysis contribute to *B abortus*–induced anemia

A red blood cell (RBC) biotinylation assay to compare the RBC lifespans of *B abortus*–treated and saline control mice (Figure 4A) demonstrated a 2.5-fold shortening of the erythrocyte lifespan in *B abortus*–treated mice, indicating that increased RBC destruction was contributing to the anemia. Erythrocyte abnormalities in *B abortus*–treated mice were most prominent at 14 days (Figure 4B), with schistocytes and RBC membrane irregularities indicative of membrane damage. However, the condition was relatively mild, as indicated by schistocytes comprising <1% of erythrocytes even at 14 days (see the next section). For comparison, in a human disorder with prominent microangiopathic hemolysis such as the hemolytic-uremic syndrome, the percentage schistocytes ranged from 2% to 9%.[29]

Microscopic examination of hematoxylin and eosin, periodic acid-Schiff, and Masson trichrome stains of liver, kidney, spleen, and pancreas sections obtained at autopsies of *B abortus*– and saline-treated mice revealed foci of thrombosis in small arteries and veins in the liver and the kidneys (supplemental Figure 2C-D), as well as in peripancreatic adipose tissue (data not shown), indicative of endothelial injury and microthrombosis that could cause microangiopathic hemolysis.

Contribution of hepcidin to *B abortus*–induced hypoferremia and anemia

We next examined the development of hypoferremia and anemia in *B abortus*–treated *Hamp*-KO. Prior to use in this study, *Hamp*-KO mice were placed for 4 weeks on an iron-restricted diet to prevent the massive iron overload characteristic of *Hamp*-KO mice, so that they were as similar as possible to WT mice except for the effect of hepcidin during inflammation in the latter. Iron-depleted *Hamp*-KO mice had similar blood hemoglobin as their WT counterparts (Figure 5A). Like WT mice, *B abortus*–treated *Hamp*-KO mice became inflamed, as indicated by increased SAA-1 mRNA levels and leukocytosis (supplemental Figure 3). Like WT mice, *Hamp*-KO mice showed erythrocyte fragments on blood smears, most prominently at 14 days (0.7 ± 0.5% of erythrocytes in WT, 0.5 ± 0.1% in

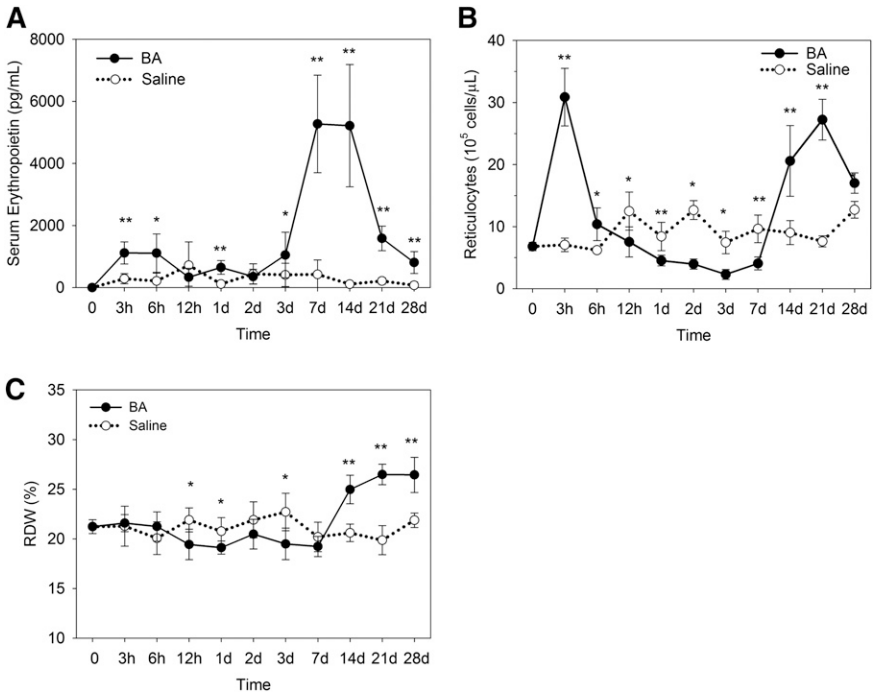

Figure 3. Suppression and recovery of erythropoiesis in *B abortus*–treated mice. (A) Serum erythropoietin concentrations in *B abortus*–treated mice increase to a peak by 7 days, with a decline approaching normal values by 28 days. (B) After the initial release of reticulocytes at 3 hours, reticulocytes decrease significantly below those of saline-treated mice from 12 hours to 7 days, followed by reticulocytosis on days 14 to 28. (C) Consistent with decreased reticulocytes in *B abortus*–treated mice, the red cell distribution width is suppressed at 12 hours to 3 days but increases by 14 days. Means ± SD are shown. $^*P < .05$ and $^{**}P < .001$ by Student *t* test or Mann-Whitney *U* test.

Hamp-KO, n = 4 mice each group, difference not significant by Student *t* test). Both *B abortus*–treated groups (*Hamp*-KO and WT) reached their hemoglobin nadir at 14 days, but the anemia of the *Hamp*-KO mice was much milder than in the WT mice (*Hamp*-KO *B abortus* Hgb 9.8 g/dL vs WT *B abortus* Hgb 6.8 g/dL; $P < .001$ by Mann-Whitney *U* test). Moreover, the *Hamp*-KO *B abortus*–treated mice recovered completely by 28 days, whereas the WT *B abortus* mice did not (*Hamp*-KO *B abortus* Hgb 15.1 g/dL vs WT *B abortus* Hgb 10.7 g/dL; $P < .001$ by Student *t* test).

As expected, compared with WT mice, serum iron in *Hamp*-KO mice remained elevated even on an iron-restricted diet that substantially depleted their iron stores (Figure 5B). Unlike WT mice, the *B abortus*–treated *Hamp*-KO mice did not develop hypoferremia, but on the contrary, showed increased serum iron. At 14 days, the *B abortus*–treated *Hamp*-KO mice had a nearly twofold increase in serum iron compared with saline-treated *Hamp*-KO mice ($P < .05$ by Mann-Whitney *U* test). Higher serum iron is likely due to increased destruction of RBCs after *B abortus* treatment and recycling of their iron content. ZPP, an index of iron-restricted erythropoiesis, changed very little in *B abortus*–treated *Hamp*-KO mice compared with WT mice (Figure 5C).

Compared with the saline *Hamp*-KO group, *B abortus*–treated *Hamp*-KO mice transiently decreased their liver iron stores at 7 and 14 days, indicating that *Hamp*-KO mice mobilized iron from stores in response to anemia. In contrast, despite anemia and increased erythropoietic activity, *B abortus*–treated WT mice had increased liver iron stores compared with their saline counterparts, suggesting that hepcidin prevented efficient mobilization of iron from the liver (Figure 5D).

Interestingly, *Hamp*-KO mice had significantly decreased survival compared with their WT counterparts (supplemental Figure 4). Thus, although hepcidin ablation was protective against the development of severe anemia and iron restriction, hepcidin deficiency or the associated iron redistribution may have impacted *B abortus*–induced inflammation or its damaging effects on tissues and organs.

Discussion

AI (also called anemia of chronic disease) is a mild to moderate, usually normocytic anemia seen in the context of infections and

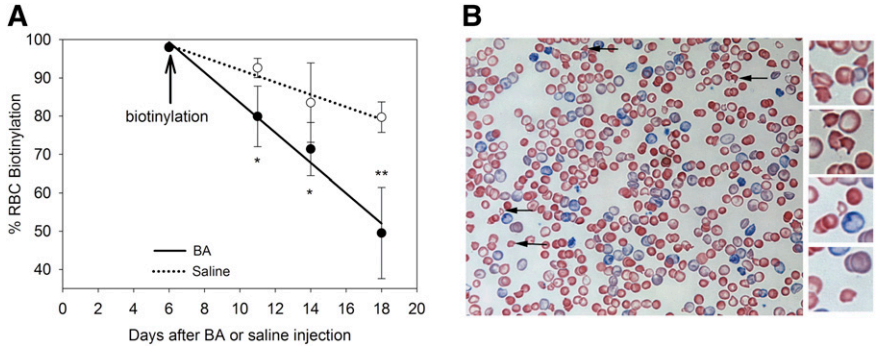

Figure 4. *B abortus*–treated mice have shortened RBC lifespan and evidence of hemolysis. (A) The RBC biotinylation assay indicates a 2.7-fold increase in RBC destruction in *B abortus*–treated mice (−4%/day vs −1.7%/day). Means ± SD. $^*P < .05$ and $^{**}P < .001$ by Student *t* test or Mann-Whitney *U* test. Overall difference between the 2 sets of measurements is significant at $P < .001$ by 2-way analysis of variance (Holm-Sidak method). (B) Peripheral blood smears of *B abortus*–injected mice 2 weeks after showing schistocytes and erythrocyte membrane irregularities, consistent with mild microangiopathic hemolysis. Arrows point to damaged erythrocytes, shown magnified in the right margin.

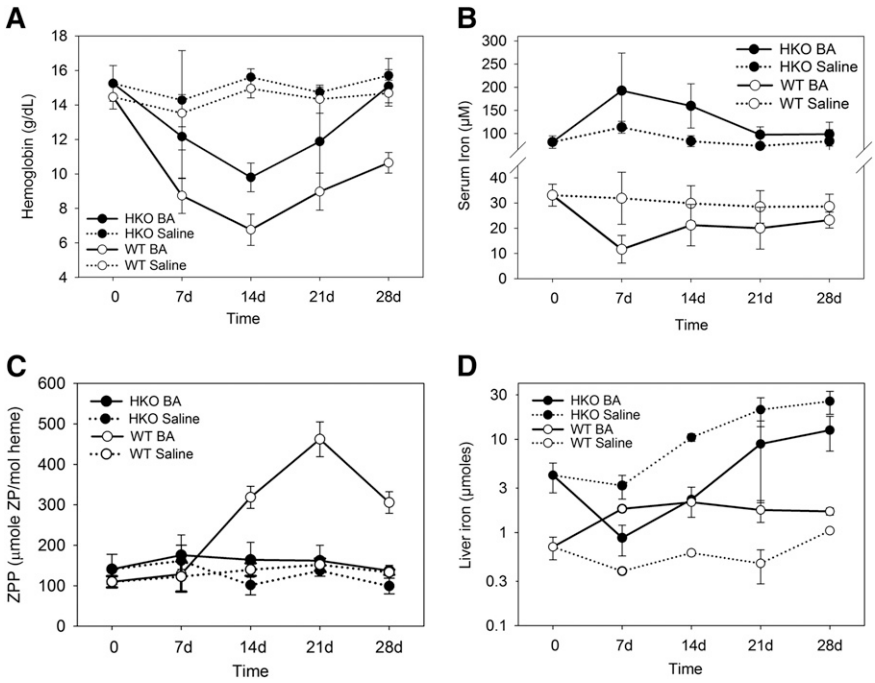

Figure 5. Hepcidin ablation attenuates *B abortus*–induced anemia and iron restriction. (A) *B abortus*–treated *Hamp*-KO mice (HKO) develop milder anemia than their WT counterparts and completely recover by 28 days. *Hamp*-KO *B abortus* vs WT *B abortus*, day 7 or 21, $P < .05$; *Hamp*-KO *B abortus* vs WT *B abortus*, day 14 or 28, $P < .001$, n = 3 to 8 per time point. (B) Unlike their WT counterparts, *B abortus*–injected *Hamp*-KO mice increase their serum iron levels. *Hamp*-KO *B abortus* vs *Hamp*-KO saline, day 14, $P < .05$; WT *B abortus* vs WT saline, days 7, 14, 21, and 28, $P < .05$. (C) *B abortus*–treated WT mice have dramatically increased RBC ZPP, indicating iron-restricted erythropoiesis, compared with the very modest increases of ZPP in *Hamp*-KO mice. (D) *B abortus*–treated *Hamp*-KO mice mobilize iron from liver iron stores, whereas their WT counterparts mildly increase their stores in the face of anemia. *Hamp*-KO *B abortus* vs *Hamp*-KO saline, day 14, $P < .001$; day 28, $P < .05$. WT *B abortus* vs WT saline, day 7 or 14, $P < .001$; day 21, $P < .05$. Means ± SD are shown. *P* value by Student *t* test or Mann-Whitney *U* test. WT data shown in A-C are identical to those from Figure 1A-B,D.

systemic inflammatory disorders including rheumatologic disorders, inflammatory bowel diseases, and malignant neoplasms.[1] In addition, chronic kidney diseases often manifest inflammation and associated features of AI. A related condition, anemia of critical illness, develops in intensive care unit settings within days.[30,31] The pathogenesis of AI is thought to involve a prominent component of inflammation-induced iron restriction, as well as impaired proliferation of erythroid precursors, resistance to erythropoietin, and shortened erythrocyte survival,[1,32] and may be further exacerbated by blood loss and iron deficiency. Progress in understanding these and additional mechanisms has been hampered by the lack of a simple and reproducible animal model that can be genetically manipulated.

In this study, we extensively characterized a mouse model of AI induced by heat-killed *B abortus*. In contrast to other mouse models of AI, where anemia was generally very mild, the *B abortus*–induced anemia results in a nadir hemoglobin that is <50% of the controls. Remarkably, the *B abortus* model is technically simple, requiring only a single injection, and it is robust and reproducible at each time point, with small standard deviations for most hematologic, iron, and inflammatory parameters measured. The model has features of both acute and chronic inflammation, as evidenced by the early SAA-1 increase and the delayed leukocytosis and hepatic perivascular infiltration of inflammatory cells.

Clinically, this subacute mouse model of moderately severe AI resembles human AI in severe infections, or in critically ill patients in intensive care units, or in patients with severe exacerbations of systemic autoimmune diseases. It remains to be tested whether lower dosing of heat-killed *B abortus* with repeated administration would result in a less severe and more chronic model, with steady-state anemia similar to classical anemia of chronic disease.

Our mouse model manifests the key mechanisms implicated in human AI, including hypoferremia and iron-restricted erythropoiesis with preserved iron stores, shortened erythrocyte lifespan, and depressed erythropoiesis. Hypoferremia developed rapidly, probably as a consequence of acute increase in hepcidin mRNA and plasma levels driven by inflammation after *B abortus* injection. Although following the initial rise hepcidin fell to control levels during the first week, this may not have been sufficiently low in the face of the developing anemia, further contributing to iron restriction. Elevated liver iron in *B abortus*–treated WT mice compared with their saline counterparts further supports the role of hepcidin in preventing effective iron mobilization for the recovery from anemia.

The shortened erythrocyte lifespan in the *B abortus* mouse model may be a consequence of macrophage activation by cytokines[32,33] and/or microangiopathic hemolysis. In support of the latter mechanism, arteriolar and venous microthrombosis was observed in multiple tissues, and fragmented red cells were apparent on blood smears. However, we did not detect the characteristic deposition of fibrin in renal glomerular capillaries, and schistocytes were relatively rare, suggesting that the condition was not severe. Increased erythrophagocytosis by inflammation-activated macrophages was documented in the companion article[34] and may well be the predominant mechanism shortening the erythrocyte lifespan.

Depressed erythropoiesis is evidenced in our model by a transient suppression of reticulocyte counts despite adequate levels of circulating erythropoietin. The blunted response of the bone marrow to the erythropoietic hormone has been seen in other inflammatory mouse models, including a turpentine-induced sterile abscess model[12] and a chronic interferon-γ (IFN-γ) overproduction model. Libregts et al[33] demonstrated that IFN-γ stimulation promotes monocytic differentiation at the expense of erythroid differentiation, suggesting that erythroid suppression may be a side effect of the increased production of defensive myeloid cells during infection. Interestingly, we observed significantly increased leukocytosis in WT *B abortus* compared with *Hamp*-KO *B abortus* mice (supplemental Figure 3B). Following recent suggestions,[33,35] we suspect that the increase in IFN-γ together with hepcidin-mediated iron restriction may promote erythropoietic suppression and a shift to leukocyte production. We speculate that delayed or inadequate shift to leukocyte production in *Hamp*-KO mice may have interfered with the neutralization of *B abortus*–associated pathogenic molecules, thereby increasing mortality. Although leukocytes are usually

thought of as cells that mediate host defense against live microbes, a leukocyte defect that delayed the breakdown of heat-killed *Aspergillus* hyphae administered to mice worsened inflammatory tissue injury.[36]

Importantly, we were able to demonstrate that our mouse model of AI was partially hepcidin-dependent. The ablation of the hepcidin gene resulted in a dramatic reduction of iron-restricted erythropoiesis and improved mobilization of iron from tissue stores. At the nadir, the *Hamp*-KO mice had hemoglobin measurements that were 3 g/dL higher than in their WT counterparts, with a faster recovery to normal values. However, the *Brucella*-treated *Hamp*-KO mice were still markedly anemic at their nadir, with a hemoglobin level 5.8 g/dL below that of controls. Although hepcidin appears to play an important role in the development of AI in this model, other mechanisms contribute significantly.

The companion paper by Gardenghi et al[34] shows strikingly similar findings with the same mouse model of AI. They observed a similar pattern of early hepcidin increases followed by marked iron-restricted anemia and a slow recovery. Using complementary studies, Gardenghi et al[34] also demonstrated erythropoietic suppression and shortened erythrocyte lifespan. Flow cytometry confirmed an absence of early erythroid progenitor cells in the bone marrow, and a biotinylation assay showed an increased rate of erythrocyte elimination in the *B abortus*–treated mice. *Hamp*-KO mice in their experiments also had a milder anemia with an accelerated recovery. Erythrocyte survival in *B abortus*–treated *Hamp*-KO mice was shortened similarly to that of WT mice. Interestingly, Gardenghi et al[34] found that the ablation of IL-6 also offered a protective effect against AI, albeit weaker than the effect of hepcidin-1 ablation.

As illustrated by its original use[17] and the current studies by us and Gardenghi et al,[34] the *B abortus* model of AI should be useful for the exploration of the mechanisms and possible treatments of AI.

Acknowledgments

The authors thank Dr Charles Lassman (Department of Pathology, UCLA) for his patient guidance in interpreting the histopathology sections. The authors also thank Drs Tara Arvedson, Barbra Sasu, and Keegan Cooke for introducing us to the mouse model described in this manuscript and for sharing the mouse hepcidin immunoassay. The authors thank all our colleagues at Xenon Pharmaceuticals for many helpful discussions that made this work possible.

This study was supported by research funding from Xenon Pharmaceuticals (to T.G. and E.N.).

Authorship

Contribution: A.K., E.F., E.V.V., E.N., and T.G. designed the studies, analyzed the data, and wrote or edited the manuscript; and A.K., E.F., S.G.P., E.V.V., and V.G. performed and analyzed the experiments.

Conflict-of-interest disclosure: T.G. and E.N. are cofounders, shareholders, and officers of Intrinsic LifeSciences, a company developing hepcidin diagnostics, and shareholders in Merganser Biotech, engaged in the development of hepcidin-based therapeutics. In the last 2 years, they have received research funding from Amgen and Xenon and were consultants for Xenon. T.G. is a consultant to Keryx. E.N. and T.G. hold patents related to the therapeutic use of hepcidin and its regulators. The remaining authors declare no competing financial interests.

Correspondence: Tomas Ganz, 37-055 CHS, Department of Medicine, UCLA, 10833 Le Conte Ave, Los Angeles, CA 90095; e-mail: tganz@mednet.ucla.edu.

References

1. Weiss G, Goodnough LT. Anemia of chronic disease. *N Engl J Med.* 2005;352(10):1011-1023.
2. Adamson JW. The anemia of inflammation/malignancy: mechanisms and management. *Hematology (Am Soc Hematol Educ Program).* 2008:159-165.
3. Park CH, Valore EV, Waring AJ, Ganz T. Hepcidin, a urinary antimicrobial peptide synthesized in the liver. *J Biol Chem.* 2001; 276(11):7806-7810.
4. Ganz T, Nemeth E. Hepcidin and iron homeostasis. *Biochim Biophys Acta.* 2012; 1823(9):1434-1443.
5. Roy CN, Mak HH, Akpan I, Losyev G, Zurakowski D, Andrews NC. Hepcidin antimicrobial peptide transgenic mice exhibit features of the anemia of inflammation. *Blood.* 2007;109(9):4038-4044.
6. De Falco L, Sanchez M, Silvestri L, et al. Iron refractory iron deficiency anemia. *Haematologica.* 2013;98(6):845-853.
7. Nemeth E, Tuttle MS, Powelson J, et al. Hepcidin regulates cellular iron efflux by binding to ferroportin and inducing its internalization. *Science.* 2004;306(5704):2090-2093.
8. Nemeth E, Rivera S, Gabayan V, et al. IL-6 mediates hypoferremia of inflammation by inducing the synthesis of the iron regulatory hormone hepcidin. *J Clin Invest.* 2004;113(9): 1271-1276.
9. Wrighting DM, Andrews NC. Interleukin-6 induces hepcidin expression through STAT3. *Blood.* 2006; 108(9):3204-3209.
10. Pietrangelo A, Dierssen U, Valli L, et al. STAT3 is required for IL-6-gp130-dependent activation of hepcidin in vivo. *Gastroenterology.* 2007;132(1): 294-300.
11. Verga Falzacappa MV, Vujic Spasic M, Kessler R, Stolte J, Hentze MW, Muckenthaler MU. STAT3 mediates hepatic hepcidin expression and its inflammatory stimulation. *Blood.* 2007;109(1): 353-358.
12. Prince OD, Langdon JM, Layman AJ, et al. Late stage erythroid precursor production is impaired in mice with chronic inflammation. *Haematologica.* 2012;97(11):1648-1656.
13. Nicolas G, Chauvet C, Viatte L, et al. The gene encoding the iron regulatory peptide hepcidin is regulated by anemia, hypoxia, and inflammation. *J Clin Invest.* 2002;110(7):1037-1044.
14. Lasocki S, Millot S, Andrieu V, et al. Phlebotomies or erythropoietin injections allow mobilization of iron stores in a mouse model mimicking intensive care anemia. *Crit Care Med.* 2008;36(8): 2388-2394.
15. Rivera S, Ganz T. Animal models of anemia of inflammation. *Semin Hematol.* 2009;46(4): 351-357.
16. Deschemin JC, Vaulont S. Role of hepcidin in the setting of hypoferremia during acute inflammation. *PLoS ONE.* 2013;8(4):e61050.
17. Sasu BJ, Cooke KS, Arvedson TL, et al. Antihepcidin antibody treatment modulates iron metabolism and is effective in a mouse model of inflammation-induced anemia. *Blood.* 2010; 115(17):3616-3624.
18. Courselaud B, Troadec MB, Fruchon S, et al. Strain and gender modulate hepatic hepcidin 1 and 2 mRNA expression in mice. *Blood Cells Mol Dis.* 2004;32(2):283-289.
19. Ramos E, Kautz L, Rodriguez R, et al. Evidence for distinct pathways of hepcidin regulation by acute and chronic iron loading in mice. *Hepatology.* 2011;53(4):1333-1341.
20. Zhang Z, Zhang F, Guo X, An P, Tao Y, Wang F. Ferroportin1 in hepatocytes and macrophages is required for the efficient mobilization of body iron stores in mice. *Hepatology.* 2012;56(3):961-971.
21. Lesbordes-Brion JC, Viatte L, Bennoun M, et al. Targeted disruption of the hepcidin 1 gene results in severe hemochromatosis. *Blood.* 2006;108(4): 1402-1405.
22. Ramos E, Ruchala P, Goodnough JB, et al. Minihepcidins prevent iron overload in a hepcidin-deficient mouse model of severe hemochromatosis. *Blood.* 2012;120(18): 3829-3836.
23. Hod EA, Francis RO, Spitalnik SL, et al. Validation and preclinical correlation of a new sandwich ELISA for measuring murine hepcidin [abstract]. *Blood.* 2012;120(21). Abstract 2100.
24. Goodnough JB, Ramos E, Nemeth E, Ganz T. Inhibition of hepcidin transcription by growth factors. *Hepatology.* 2012;56(1):291-299.
25. Brugnara C. Reticulocyte cellular indices: a new approach in the diagnosis of anemias and monitoring of erythropoietic function. *Crit Rev Clin Lab Sci.* 2000;37(2):93-130.
26. Wong SS, Qutishat AS, Lange J, Gornet TG, Buja LM. Detection of iron-deficiency anemia in hospitalized patients by zinc protoporphyrin. *Clin Chim Acta.* 1996;244(1):91-101.

27. Hagihara K, Nishikawa T, Isobe T, Song J, Sugamata Y, Yoshizaki K. IL-6 plays a critical role in the synergistic induction of human serum amyloid A (SAA) gene when stimulated with proinflammatory cytokines as analyzed with an SAA isoform real-time quantitative RT-PCR assay system. *Biochem Biophys Res Commun*. 2004;314(2):363-369.

28. Pak M, Lopez MA, Gabayan V, Ganz T, Rivera S. Suppression of hepcidin during anemia requires erythropoietic activity. *Blood*. 2006;108(12): 3730-3735.

29. Saigo K, Jiang M, Tanaka C, et al. Usefulness of automatic detection of fragmented red cells using a hematology analyzer for diagnosis of thrombotic microangiopathy. *Clin Lab Haematol*. 2002;24(6): 347-351.

30. Vincent JL, Baron JF, Reinhart K, et al; ABC (Anemia and Blood Transfusion in Critical Care) Investigators. Anemia and blood transfusion in critically ill patients. *JAMA*. 2002;288(12): 1499-1507.

31. Hayden SJ, Albert TJ, Watkins TR, Swenson ER. Anemia in critical illness: insights into etiology, consequences, and management. *Am J Respir Crit Care Med*. 2012;185(10):1049-1057.

32. Cartwright GE. The anemia of chronic disorders. *Semin Hematol*. 1966;3(4):351-375.

33. Libregts SF, Gutiérrez L, de Bruin AM, et al. Chronic IFN-γ production in mice induces anemia by reducing erythrocyte life span and inhibiting erythropoiesis through an IRF-1/PU.1 axis. *Blood*. 2011;118(9):2578-2588.

34. Gardenghi S, Renaud TM, Meloni A, et al. Distinct roles for hepcidin and interleukin-6 in the recovery from anemia in mice injected with heat-killed *Brucella abortus* [published online ahead of print December 19, 2013]. *Blood*. doi:10.1182/blood-2013-08-521625.

35. Richardson CL, Delehanty LL, Bullock GC, et al. Isocitrate ameliorates anemia by suppressing the erythroid iron restriction response. *J Clin Invest*. 2013;123(8):3614-3623.

36. Morgenstern DE, Gifford MA, Li LL, Doerschuk CM, Dinauer MC. Absence of respiratory burst in X-linked chronic granulomatous disease mice leads to abnormalities in both host defense and inflammatory response to Aspergillus fumigatus. *J Exp Med*. 1997;185(2): 207-218.